LCLS-II Technical Note

RF Beam Spreader Options for LCLS-II

LCLS-II TN-13-05

12/6/2013

Jean Delayen, Subashini De Silva, Rocio Olave, Todd Satogata, Geoff Krafft

(1) Introduction

A three-way separator system is required in the LCLS–II as shown in **Figure 1**, in separating and transporting the beam to the two undulators. The rf parameters of the deflecting cavities are given in **Table 1**. A transverse voltage of 4 MV is considered in all the deflecting cavity options designing to more aggressive requirement with a net deflection of 1 mrad. Three rf cavity design options are presented at an operating frequency of 325 MHz.

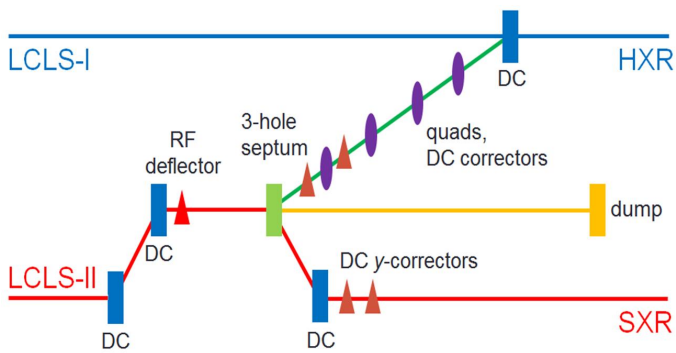

Figure 1. LCLS-II 3-way beam spreader.

Table 1. RF spreader requirements.

Parameter	Symbol	Value	Unit
Electron energy	E_f	4.0	GeV
Angle of deflection	θ_{def}	0.75 / 1.0	mrad
Transverse voltage	V_T	3.0 / 4.0	MV
RF frequency	f	325	MHz

(1) Superconducting RF-Dipole Cavity Option

The superconducting rf-dipole cavity [1] shown in **Figure ~~Figure~~ 2** is the preliminary design optimized for 325 MHz. The geometry is favorable at low operating frequencies and has attractive properties such as low surface fields and high shunt impedance. The rf properties depend on fewer parameters as shown in **Figure 2**. Low and balanced surface fields are achieved by optimizing the bar height and angle. **Figure 3** shows the rf fields and surface fields of the rf dipole geometry. Field non-uniformity is reduced by increasing the bar height, which also increases the peak surface magnetic field to transverse electric field ratio (B_P/E_T) and shunt impedance (R_TR_S). A higher degree of field uniformity across the beam aperture, with a low B_P/E_T ratio, is achievable by curving the trapezoidal-shaped loading elements around the beam aperture region [2]. The fundamental deflecting mode is the lowest mode in this geometry with widely separated higher order modes, with the frequency of the next neighbor HOM (508 MHz) greater than 1.5 times the frequency of the fundamental operating mode [3] as shown in **Figure 4**.

Formatted: Font: Bold

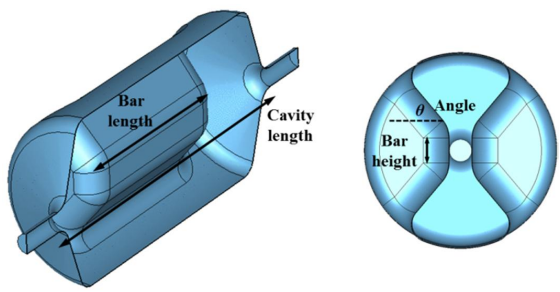

Figure 2. Supercondcuting rf-dipole cavity, showing optimization parameters for LCLS-II spreader design.

The preliminary design optimization is carried out with a beam aperture of 40 mm; this is the minimum for cavity processing, and is sufficiently large in comparison to the undulator apertures. Depending on longitudinal and transverse impedance requirements, the aperture can be further modified, where small beam apertures are favorable in achieving low peak surface field ratios and higher shunt impedance.

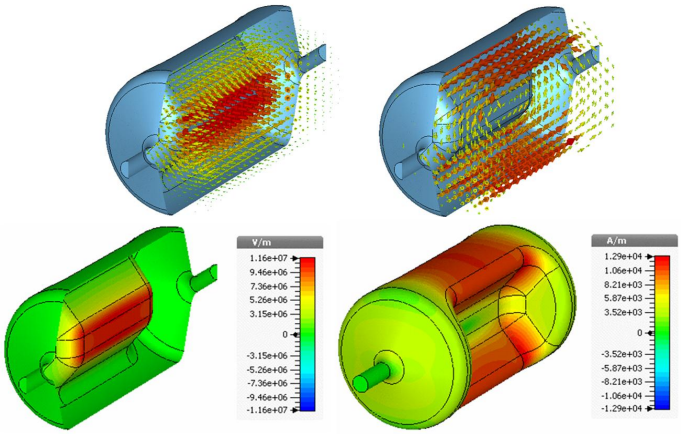

Figure 3. Electric field (top left), magnetic field (top right), surface electric field (bottom left) and surface magnetic field (bottom right) of the superconducting rf-dipole cavity (At 1 J).

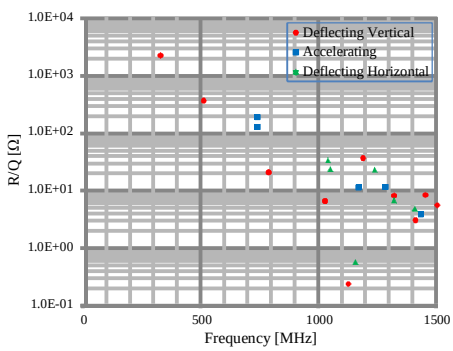

Figure 4. Higher order mode spectrum.

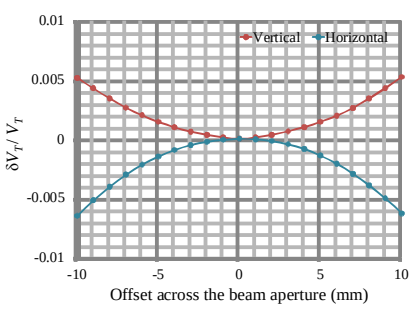

Figure 5. Normalized transverse voltage variation across the beam aperture.

Table 2. RF parameters of the LCLS-II beam separator superconducting rf-dipole cavity.

Parameter	Symbol	Value	Unit
Frequency	f	325	MHz
Frequency of nearest HOM		508	MHz
$\lambda/2$ of π mode	$\lambda/2$	461.2	mm
Beam aperture	d_{apt}	40	mm
Cavity length (iris to iris)	L_{cav}	696	mm
Cavity diameter	D_{cav}	340	mm
Bar height		44	mm
Bar length		407	mm
Angle		50	deg
Deflecting voltage (At $E_T^* = 1$ MV/m)	V_T^*	0.46	MV
Peak electric field (At $E_T^* = 1$ MV/m)	E_P^*	2.6	MV/m
Peak magnetic field (At $E_T^* = 1$ MV/m)	B_P^*	3.6	mT
B_P / E_P		1.4	mT/ (MV/m)
Stored energy (At $E_T^* = 1$ MV/m)	U^*	0.049	J
Geometrical factor	$G = QR_S$	91.5	Ω
Transverse $[R/Q]$	$[R/Q]_T$	2133	Ω
$R_T R_S$	$R_T R_S$	1.95×10^5	Ω^2
Transverse voltage	V_T	4.0	MV
Peak electric field (At $V_T = 4$ MV)	E_P	23	MV/m
Peak magnetic field (At $V_T = 4$ MV)	B_P	32	mT
Operating temperature		2.0 / 4.2	K
Surface Resistance ($R_{res} = 10$ nΩ)	R_S	10.9 / 58.7	nΩ
Unloaded quality factor	Q_0	8.4 / 1.6	$\times10^9$
RF power (At $V_T = 4$ MV)	P_{diss}	0.9 / 4.8	W
Loaded quality factor ($\Delta x = 5$ mm and $I_{avg} = 0.02$ mA)	Q_L	5.5×10^6	
Loaded bandwidth		59	Hz
Compensation for beam loading ($\Delta x = 5$ mm and $I_{avg} = 0.02$ mA)		1.4	kW

A smaller bar height gives low peak magnetic field ratio (B_P/E_T) and high shunt impedance (R_TR_S), but increases peak electric field ratio (E_P/E_T) and the field non-uniformity across the beam aperture. The small beam aperture selected at the low frequency of 325 MHz contributes to low peak surface field ratios of E_P/E_T=2.6 and B_P/E_T=3.6 mT/(MV/m), with a peak field-balancing ratio of B_P/E_P=1.4 mT/(MV/m). Ideally a peak field-balancing ratio of ~2.0 mT/(MV/m) is preferred [1], however it is not a critical parameter at low peak operating fields. Hence the design is optimized with sufficiently higher bar height, in order to improve the field non-uniformity without degrading the shunt impedance drastically. This provides with a low E_P/E_T and a slightly higher B_P/E_T ratio. The transverse voltage variation across the beam aperture is shown in **Figure** ~~**Figure**~~ **5** for offsets up to ±1 cm.

Formatted: Font: Bold

The required transverse voltage (V_T) of 4.0 MV can be achieved by one cavity with peak surface electric field of 23 MV/m and peak surface magnetic field of 32 mT, as given in Table 2. The rf power requirements for both 2.0 K and 4.2 K cryogenic temperatures are presented in Table 2, assuming a residual surface resistance (R_{res}) of 10 nΩ. The cavity can be easily operated at 4.2 K, considering the rf power required to achieve the transverse voltage of 4.0 MV. This requires liquid He availability at the rf spreader system, supplied either by a transfer line or separate refrigeration.

As shown in **Figure 4**, the fundamental deflecting mode is well-separated from the higher order modes. With adequately damped higher order modes, the beam loading compensation is determined for the fundamental operating mode. The loaded quality factor was determined considering a beam offset of Δx=5 mm where the transverse voltage variation is as low as $\delta V_T = 0.002V_T$. Additional rf power required in beam loading compensation for the average beam current (I_0) of 0.02 mA is 1.4 kW, and varies linearly with beam current. The resultant loaded bandwidth is ~60 Hz, which is wide considering the effects due to microphonics (Δf_m = 30 Hz). For high beam currents with strict impedance requirements HOMs could be successfully damped with either waveguide or coaxial-filter type HOM dampers [4, 5].

Multipacting conditions are expected to be processed easily as demonstrated in the proof-of-principle rf-dipole cavities of 400 MHz and 499 MHz [6, 7].

(2) Normal Conducting RF-Dipole Cavity Option

The normal conducting rf-dipole cavity was designed by scaling the 139 MHz design proposed for NGLS [8] with a beam aperture of 25 mm, in achieving improved rf properties and simpler rf processing required for normal conducting cavities. The design was adapted from the superconducting rf-dipole cavity by increasing the bar length significantly as shown in **Figure 6**. This gives an additive contribution from the magnetic field, contrary to that of the superconducting rf-dipole cavity where the small contribution from the magnetic fields opposes the net deflection.

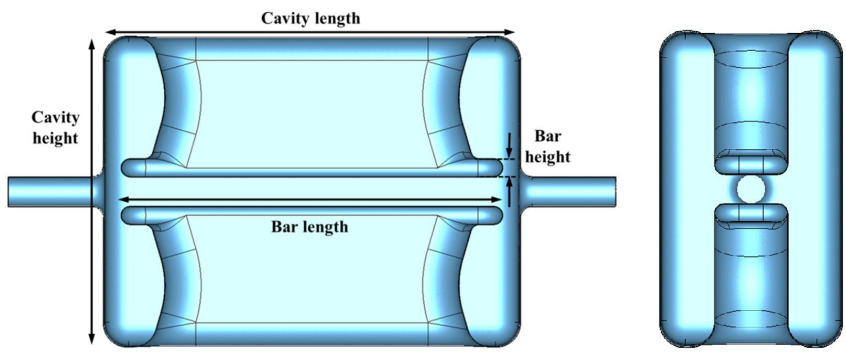

Figure 6. Normal conducting rf-dipole cavity with cross section, showing optimization parameters for LCLS-II spreader design.

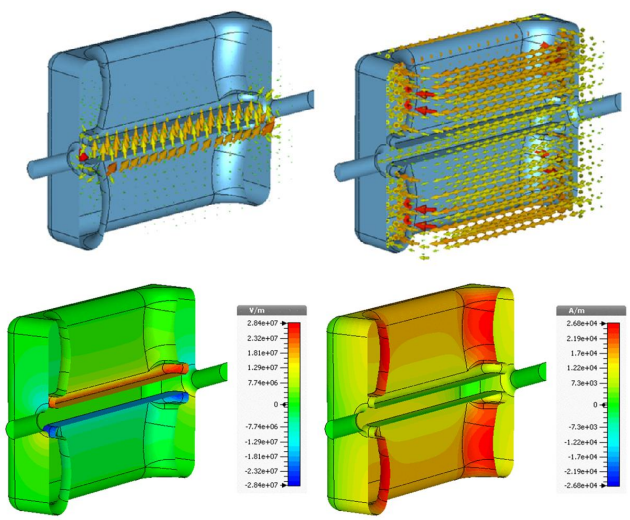

Figure 7. Electric field (top left), magnetic field (top right), surface electric field (bottom left) and surface magnetic field (bottom right) of the normal conducting rf-dipole cavity (At 1 J).

Table 3. RF parameters of the LCLS-II beam separator normal conducting rf-dipole cavity.

Parameter	Symbol	Value	Unit
Frequency	f	325	MHz
Frequency of nearest HOM		518	MHz
$\lambda/2$ of π mode	$\lambda/2$	461.2	mm
Beam aperture	d_{apt}	25	mm
Cavity length (iris to iris)	L_{cav}	370	mm
Cavity height	H_{cav}	261	mm
Cavity width	W_{cav}	150	mm
Bar length		305	mm
Bar height		15	mm
Deflecting voltage (At $E_T^* = 1$ MV/m)	V_T^*	0.46	MV
Peak electric field (At $E_T^* = 1$ MV/m)	E_P^*	3.2	MV/m
Peak magnetic field (At $E_T^* = 1$ MV/m)	B_P^*	3.8	mT
Stored energy (At $E_T^* = 1$ MV/m)	U^*	0.013	J
Geometrical factor	$G = QR_S$	48.3	Ω
Transverse $[R/Q]$	$[R/Q]_T$	8367	Ω
R_TR_S	R_TR_S	4.0×10^5	Ω^2
Transverse shunt impedance	R_T	86	MΩ
Transverse voltage	V_T	4.0	MV
Peak electric field (At $V_T = 4$ MV)	E_P	28	MV/m
Peak magnetic field (At $V_T = 4$ MV)	B_P	33	mT
Surface resistance (OFE Cu – $\sigma = 5.8\times10^7$ S/m)	R_S	4.7	mΩ
Unloaded quality factor	Q_0	1.03×10^4	
RF power (At $V_T = 4$ MV)	P_{diss}	186	kW
Peak dP_{diss} / dA (At $V_T = 4$ MV)		158	W/cm^2
No. of cavities		6	
RF Power per cavity (At $V_T = 0.67$ MV)	P_{diss}	5.2	kW
Peak dP_{diss} / dA per cavity (At $V_T = 0.67$ MV)		4.4	W/cm^2

The rf fields and surface fields of the preliminary normal conducting rf-dipole design are shown in **Figure 7** with the rf properties given in Table 3.

The transverse shunt impedance is increased significantly with an increase in the transverse [R/Q] in the normal conducting design. The longer bar length supports higher transverse [R/Q] due to the resultant increase in the effective deflecting length. This change also reduces the field non-uniformity across the beam aperture. The bar height is required to be shorter to gain a higher transverse [R/Q]; it is 15 mm in the current design. This results in a high surface electric field at the edges of the bars as shown in **Figure 7**. The high surface electric field present at the edges of the bars and the high surface magnetic field at the sides of the bars as shown in **Figure 7** are reduced by substantial rounding. The peak surface electric field (E_P^*) at a transverse electric field of E_T=1 MV/m is 0.8×Kilpatric limit at 325 MHz, and hence does not exceed the Kilpatrick criterion.

The beam aperture of the preliminary design is chosen to be 25 mm due to the strong relation of aperture size to the transverse shunt impedance (R_T). The increase in the aperture drastically reduces R_T. The current design has a transverse shunt impedance of 86 MΩ that requires 186 kW of total rf power to achieve the required transverse deflection of 4.0 MV, driven by one cavity. This requires 6 cavities, at a power dissipation of 5.2 kW per cavity and the corresponding use of longitudinal beam line space. The curved surfaces of the bars significantly improves the surface magnetic field and therefore has cooling requirements as low as 4.4 W/cm^2 per cavity.

(3) Normal Conducting 4-Rod Cavity Option

The single cell 4-rod cavity design is adapted from the 499 MHz 4-rod rf separator cavity that is currently in operation in CEBAF at Jefferson Lab [9, 10]. The preliminary design was analyzed with a beam aperture of 25 mm.

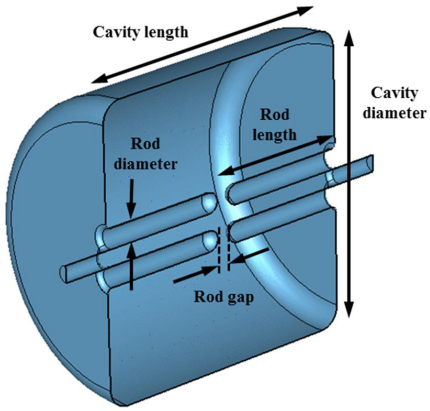

Figure 8. Normal conducting 4-rod cavity, showing optimization parameters for LCLS-II spreader design.

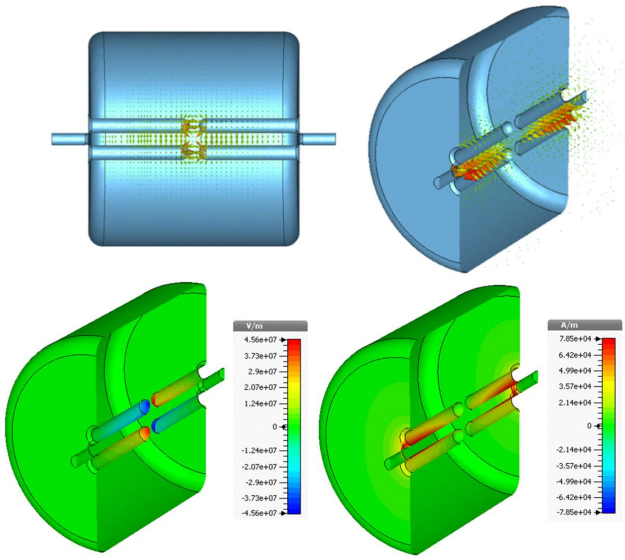

Figure 9. Electric field (top left), magnetic field (top right), surface electric field (bottom left) and surface magnetic field (bottom right) of the normal conducting 4-rod cavity (At 1 J).

The rf fields and surface fields of the single cell normal conducting 4-rod cavity design are shown in **Figure 9** with the rf properties given in **Table** 4.

Table 4. RF parameters of the LCLS-II beam separator normal conducting 4-rod cavity.

Parameter	Symbol	Value	Unit
Frequency	f	325	MHz
Frequency of LOM		226	MHz
Frequency of nearest HOM		349	MHz
Beam aperture	d_{apt}	25	mm
Cavity length (iris to iris)	L_{cav}	450	mm
Cavity diameter	D_{cav}	444	mm
Rod length		207.5	mm
Rod diameter		30.7	mm
Gap between rods		20.1	mm
Deflecting voltage (At $E_T^* = 1$ MV/m)	V_T^*	0.46	MV
Peak electric field (At $E_T^* = 1$ MV/m)	E_P^*	3.4	MV/m
Peak magnetic field (At $E_T^* = 1$ MV/m)	B_P^*	7.2	mT
Stored energy (At $E_T^* = 1$ MV/m)	U^*	5.4	mJ
Geometrical factor	$G = QR_S$	37.3	Ω
Transverse $[R/Q]$	$[R/Q]_T$	1.9×10^4	Ω
R_TR_S	R_TR_S	7.2×10^5	Ω^2
Transverse shunt impedance	R_T	153	MΩ
Transverse Voltage	V_T	4.0	MV
Peak electric field (At $V_T = 4$ MV)	E_P	29	MV/m
Peak magnetic field (At $V_T = 4$ MV)	B_P	63	mT
Surface resistance (OFE Cu – $\sigma = 5.8\times10^7$ S/m)	R_S	4.7	mΩ
Unloaded quality factor	Q_0	8.0×10^3	
Total RF Power (At $V_T = 4$ MV)	P_{diss}	104.4	kW
Total Peak dP_{diss} / dA (At $V_T = 4$ MV)		583	W/cm^2
No of cavities		4	
RF Power per cavity (At $V_T = 1$ MV)	P_{diss}	6.5	kW
Peak dP_{diss} / dA per cavity (At $V_T = 1$ MV)		36	W/cm^2

The longitudinal size of the cavity is governed primarily by the rod length that is related to the wavelength of the cavity, and is approximately λ/4 for each rod. The orientation of the rods have higher surface electric fields at the tips of the rods and high surface magnetic fields at rod ends connecting to the end plates as shown in **Figure 9**. The design is optimized to be within the Kilpatrick criterion, with a peak surface electric field of 0.84×Kilpatrick limit at 325 MHz and E_T= 1 MV/m. High surface magnetic field at the ends of the parallel rods can be further reduced with improved rod geometries.

The deflecting mode is not the lowest mode in this geometry and has a lower order mode at 226 MHz present in the geometry.

A large beam aperture size severely reduces transverse shunt impedance [11] compared to that in the normal conducting rf-dipole cavity. An identical beam aperture of 25 mm is chosen in comparison with the previous design option; however the smaller aperture is preferred to achieve higher shunt impedance.

The 4-rod cavity has higher transverse shunt impedance (153 MΩ) compared to the normal conducting rf-dipole cavity, reducing the total power required to 104 kW in achieving the total deflection of 4.0 MV, operating with one cavity. The net transverse voltage requirement of 4.0 MV can be possibly achieved by 4 cavities, with a power dissipation of 6.5 kW per cavity. However the resulting design has a high peak surface magnetic field ratio (B_P^*) due to high surface magnetic field at the rod ends, requires a higher cooling requirement of 36 W/cm^2 per cavity, compared to the normal conducting rf-dipole cavity.

The 499 MHz normal conducting 4-rod cavities installed for the Jefferson Lab 12 GeV upgrade uses 2 cell designs [10] and have been modified to incorporate a parallel cooling mechanism [12]. These existing cavities have achieved a maximum rf power of 5.2 kW and are limited by the cooling of the input power coupler; consequently a higher rf power can possibly be achieved with an improved power coupler. In addition the existing cavities provide voltage ($\delta V_T/V_T$) and deflection ($\delta\theta_{def}/\theta_{def}$) stability of 0.1% each [12]. A similar 325 MHz 2-cell design is capable of delivering higher shunt impedance and will lower the power requirements.

Summary

Preliminary analyses of three possible deflecting cavity design options for the LCLS-II spreader are presented. The superconducting rf-dipole cavity option requires only one cavity to meet the design requirement of 4.0 MV, with a low rf power consumption of 5 W at 4.2 K.

The comparison between the two normal conducting cavity options shows that the total power requirements are lower in the 4-rod cavity option to that of the normal conducting rf-dipole cavity. The 4-rod cavity option requires fewer cavities (4 cavities) compared to that of the normal conducting rf-dipole cavity, which requires 6 cavities. The number of cavities in the normal conducting 4-rod cavity option can be reduced in adapting a 2-cell design as was done for the CEBAF 12 GeV upgrade.

References

1 S. U. De Silva and J. R. Delayen, Phys. Rev. ST Accel. Beams 16, 012004 (2013).

2 S. U. De Silva, J. R. Delayen, "Multipole Field Effects for the Superconducting Parallel-Bar Deflecting/Crabbing Cavities", in Proceedings of 2012 Linear Accelerator Conference, Tel-Aviv, Israel, p. 981.

3 S. U. De Silva, J. R. Delayen, "Analysis of HOM Properties of Superconducting Parallel-Bar Deflecting/Crabbing Cavities", in Proceedings of 2011 Conference of RF Superconductivity, Chicago, Illinois, p. 135.

4 Z. Li, L. Ge, J. R. Delayen, S. U. De Silva, "HOM Damping Coupler Design for the 400 MHz RF-Dipole Compact Crab Cavity for the LHC HiLumi Upgrade", in Proceedings of 2013 International Particle Accelerator Conference, Shanghai, China, WEPWO072.

5 Z. Li, ""HOM and FPC Coupler for LHC Crab Cavity", LHC Crab Cavity Engineering Meeting, Fermilab, December, 2012.6 S. U. De Silva and J. R. Delayen, Phys. Rev. ST Accel. Beams 16, 082001 (2013).

7 S. U. De Silva, J. R. Delayen, "Superconducting RF-Dipole Deflecting and Crabbing Cavities", in Proceedings of 2013 Conference on RF Superconductivity, Paris, France, p. 2450.

8 T. Luo, D. Summers, D. Li, "Design of a Normal Conducting RF-dipole Deflecting Cavity", in Proceedings of the 2013 International Particle Accelerator Conference, Shanghai, China, WEPFI091.

9 C.W. Leemann, C. G. Yao, "A Highly Effective Deflecting Structure" in Proceedings of the 1990 Linear Accelerator Conference, Albuquerque, New Mexico, p. 232

10 A. Krycuk, J. Fugitt, A. Johnson, R. Kazimi, L. Turlington, "Construction of the CEBAF RF Separator", in Proceedings of the 1993 Particle Accelerator Conference, Washington, D.C., p. 939.

11 S. U. De Silva, C. Hovater, M. Spata, M. Wissmann, "11 GeV Normal Conducting Separator Cavity Power Requirements", JLAB-TN-11-009, March, 2011.

12 C. Hovater, G. Arnold, J. Fugitt, L. Harwood, R. Kazimi, G. Lahti, J. Mammosser, R. Nelson, C. Piller, L. Turlington, "The CEBAF RF Separator System", in Proceedings of the 1996 Linear Accelerator Conference, Geneva, Switzerland, p. 77.

13 S. Ahmed, C. Hovater, G. A. Krafft, J. D. Mammosser, M. Spata, M. J. Wissmann, "High Power Test of RF Separator For 12 GeV Upgrade of CEBAF at Jefferson Lab", in Proceedigns of the 2012 International Particle Accelerator Conference, New Orleans, Louisiana, p. 4032.

14 C. Hovater, Private Communication.